Asian Journal of Chemistry; Vol. 32, No. 6 (2020), 1515-1519

ASIAN JOURNAL OF CHEMISTRY

https://doi.org/10.14233/ajchem.2020.22586

Influence of Nitridation on Structural and Photoluminescence Behaviour of $CaZrO_3:Eu^{3+}$ Nanophosphors

S.G. Prasanna Kumar[1,2,3], Nagaraju Kottam[2], R. Hari Krishna[2,*], M.N. Chandra Prabha[4], R. Preetham[5], Santosh Behara[6] and Tiju Thomas[6]

[1]Research and Development Centre, Bharathiar University, Coimbatore-641046, India
[2]Department of Chemistry, M.S. Ramaiah Institute of Technology, Bangalore-560054, India
[3]Department of Chemistry, M.S. Ramaiah college of Arts Science and Commerce, Bangalore-560054, India
[4]Department of Biotechnology, M.S. Ramaiah Institute of Technology, Bangalore-560054, India
[5]Department of Civil Engineering, M.S. Ramaiah Institute of Technology, Bangalore-560054, India
[6]Department of Metallurgical and Materials Engineering, Indian Institute of Technology Madras, Chennai-600036, India

*Corresponding author: E-mail: rhk.chem@msrit.edu

Received: 11 December 2019; *Accepted*: 17 April 2020; *Published online*: 30 May 2020; AJC-19906

$Ca_{1-x}ZrO_3:xEu^{3+}$ (x = 0.05) phosphors have been prepared by using the low temperature solution combustion synthesis. The prepared nano phospors are well characterized by powder X-ray diffraction, scanning electron microscopy, Fourier infrared spectroscopy and transmission electron spectroscopy. PXRD results showed orthorhombic phase and SEM images showed porous agglomerated morphology. Influence of nitridation on structural and photoluminescence properties of the phosphor were investigated for wide range of nitridation time. The photoluminescence (PL) intensity was found to vary with nitridation with small shift in the photoluminescence emission peaks. The probable reasons for the variation of photoluminescence with nitridation are discussed.

Keywords: $CaZrO_3$, Solution combustion, Nitridation, Photoluminescence.

INTRODUCTION

White LEDs, owing to their excellent properties like brightness, durability, energy efficiency, eco-friendly, *etc*. have emerged as the new generation clean and energy saving technology in solid-state lighting devices. However, white light obtained by the combination of three distinct LEDs has major disadvantage of high production costs. Research on novel white LEDs combining suitable light emitting phosphors has therefore gained momentum [1]. Commercial WLEDs currently use blue-emitting GaN chip combined with yellow emitting YAG-doped Ce^{3+} phosphor [2]. However, because of lack of red component, these LEDs suffer low colour rendering index (RA < 80) and high correlated colour temperature (CCT > 6000 K). Development of novel efficient red phosphors with broad excitation band, which can produce high quality warm white-light emission LEDs, is therefore an area of current research interest.

In this context, rare earth (RE) doped with inorganic phosphor hosts having excellent red emissions have been vastly explored. Xiao *et al*. [3] have demonstrated enhanced red emission of Eu^{3+} doped ZnO phosphor compared to undoped phosphor. Role of Sm^{3+} activator in enhancing the photoluminescence of red light emitting phosphors, Sr_2CeO_4 and $Sr_3Sc(PO_4)_3$ has been reported by Monika *et al*. [4] and Ma & Liu [5]. Efficient red phosphors with Pr^{3+} as luminophore has also has been reported [6,7]. Despite several reported studies, Eu^{3+} still continues to be an extensively researched activator for red phosphors [8].

Eu^{3+} doped red phosphors exhibit intense emission band at ~600 nm *via* the $^5D_0 \rightarrow {}^7F_2$ transition [9]. However, commercial application of these phosphors are limited owing to poor excitation of $^5D_0 \rightarrow {}^7F_2$ transition by the near ultraviolet LEDs and low colour purity due to broad emission band resulting from 4*f*-5*d* transitions [10]. Red phosphors also have problems associated with low brightness and chemical instability. Lumi-

nescent properties of doped phosphors depend on host crystal lattice structure and chemical environment of the dopant.

In recent years, nitride-based red phosphors, due to high thermal and chemical stability and interesting photoluminescence properties have received considerable attention. Nitrogen ions when compared to oxygen ions, show larger covalency and exhibit nephelauxetic effect. The resulting stable structure with lager crystal field splitting leads to significant red-shifted luminescence [11].

The charge transfer band of Eu^{3+}–N^{3-} is expected to match NUV-LED chips due to the big covalency of N^{3-} ions, indicating that Eu^{3+} ions can easily obtain the electron from the N^{3-} ions. Hoppe *et al.* [12] have reported significant red-shift in the excitation and emission of Eu^{2+} in $Ba_2Si_5N_8$, resulting in orange emission colour. Thermal quenching characteristic of the nitride phosphor was better compared to conventional oxide phosphors in $CaAlSiN_3$:Eu^{2+} [13]. Improved photoluminescence and after-glow with high reflectance by NH_3 treated $CaTiO_3$:Pr^{3+} was attributed to decreased concentration of oxygen excesses and lattice strain relaxation [14]. Nitride phosphors with significant red shift luminescence, high conversion efficiency and better thermal quenching characteristics are very suitable as down-conversion materials in WLEDs. Kate *et al*. [15] observed higher absorption and emission energy with increase in Si/N ratio in Eu^{2+} doped nitridosilicates. Increase in Si/N ratio increases N by Si coordination number leading to less negative effective charge on N atom and increase in bandgap. This results in reduced covalency of Eu-N bonds, weak nephelauxetic effect and reduction of crystal field splitting of the 5*d*-levels [15].

Oxide-based phosphors such as Y_2O_3, Dy_2O_3, ZrO_2, $CaAl_2O_4$, $CaTiO_3$, $CaSiO_3$, *etc*. due to their excellent thermal and chemical stability, ease of synthesis and non-hazardous nature have emerged as a preferred choice in WLEDs. Many inorganic hosts have been extensively studied for their luminescent properties [16-18]. Calcium zirconate ($CaZrO_3$), with high chemical and thermal stability, is a potential material for futuristic LED applications. Few researchers have explored the luminescence behaviour of trivalent lanthanide ions such as Eu^{3+}, Er^{3+}, Tm^{3+}, Tb^{3+}, Gd^{3+} and Sm^{3+} in $CaZrO_3$ [19,20]. Photoluminescence behaviour of Eu^{3+} doped $CaZrO_3$ has been discussed in our earlier studies [19]. Influence of nitridation on the luminescence behaviour of Eu^{3+} doped $CaZrO_3$ is not been reported. The present study reports the influence of nitridation on structural and photoluminescence behaviour of $CaZrO_3$:Eu^{3+} nanophosphors.

EXPERIMENTAL

The precursors used in this work for reactions were of analytical grade (Merck Ltd.) and no further purification process was carried out whatsoever. The reactants used were calcium nitrate ($Ca(NO_3)_2{\cdot}6H_2O$, 99.99%), zirconium nitrate ($ZrO(NO_3)_2{\cdot}xH_2O$, 99.99%), europium oxide (Eu_2O_3, 99%), glycine ($C_2H_5NO_2$, 99%), nitric acid and ammonia.

In the present study, nano $CaZrO_3$: Eu was synthesized with different nitrogen doping concentrations. Firstly, synthesis of $Ca_{0.95}ZrO_3$: $Eu_{0.05}$ was carried out by adopting a simple solution combustion route. Stoichiometrically calculated amounts of calcium nitrate and zirconium nitrate was added into a crystallization dish and 20 mL distilled water was used to dissolve the contents in the dish until a transparent solution was obtained. Calculated amount of europium oxide is converted to its nitrate form. Further the quantity of fuel (in this case glycine) was calculated in terms of a ratio of fuel to oxidizer based on the oxidizing and reducing valencies. The calculated amount of glycine was then added to the solution and fully dissolved. The dish was then placed inside a muffle furnace, which was preheated to a temperature of about 500 ± 10 ºC. The mixture initially undergone dehydration at that temperature. It then was observed to begin with small ignitions by the fuel and immediately result in a flame throughout the dish. Once the flames ceases and the combustion was complete, then fluffy white products of $CaZrO_3$ were obtained and then calcined for 3 h at 700 ºC. The material wass further processed to undergo nitridation in a nitridation chamber at elevated temperatures with ammonia to obtain nitrogen doping in $CaZrO_3$. The variation in the different set of $CaZrO_3$ doped with nitrogen is defined with respect to the subjected time of exposure $CaZrO_3$ in the nitridation chamber (0, 20, 40, 60, 80 and 100 min).

Characterizations: X-ray diffraction (XRD) studies were performed for the powder samples using a Shimadzu 7000 diffractometer with $\lambda = 1.54$ nm using Cu*K*α. Fourier transform infrared (FTIR) spectroscopy studies for the same samples were recorded using a Perkin-Elmer Rx1 instrument. Imaging for this work was carried out by Scanning electron microscopy technique using a JEOL (JSM-840A) setup. $CaZrO_3$ being an insulating material is required to be coated with gold for the purpose of electron micrography. Analysis based on transmission electron microscopy was done using micrographs obtained from a Hitachi H-8100 (LaB6 filament, accelerating voltage up to 200 kV). Photoluminescence (PL) studies was carried out with a Jobin-Yvon Spectro fluorimeter (Fluorolog-3), which uses a xenon lamp (450 W) as an excitation source.

RESULTS AND DISCUSSION

XRD analysis: XRD patterns of the calcined samples were recorded post nitridation and are shown Fig. 1. The graphs of all the samples exhibit a clear orthorhombic phase as observed and can be indexed with the JCPDS card No. 35-0790. A pure phase of $CaZrO_3$ observed from the diffraction patterns with no impurities. The doping of Eu^{3+} can be substituted in two possible cation sites based on the percentage acceptable ionic radius calculations where Eu^{3+} occupied the Ca^{2+} position [19]. There exists no change in the crystal structure however, the patterns show a negligible amount of shift in the peaks of the samples, which could be due to the different N-doping concentrations, a similar observation is made by Sethi *et al*. [20]. In the highest concentration of N doping, there exists an additional peak at ~ 29º, this result is similar to Cole *et al*. [21], where it also discussed as an additional peak being present in higher N concentration doping.

FTIR analysis: Fourier transform infrared spectra (Fig. 2) was used to analyze the purity and phase formation. A sharp stretching band at ~ 545 cm^{-1} is observed, which is a characteristic band of $CaZrO_3$. The peak at ~ 3462 cm^{-1} corresponds to the adsorbed water, this is a common observation in the nano-

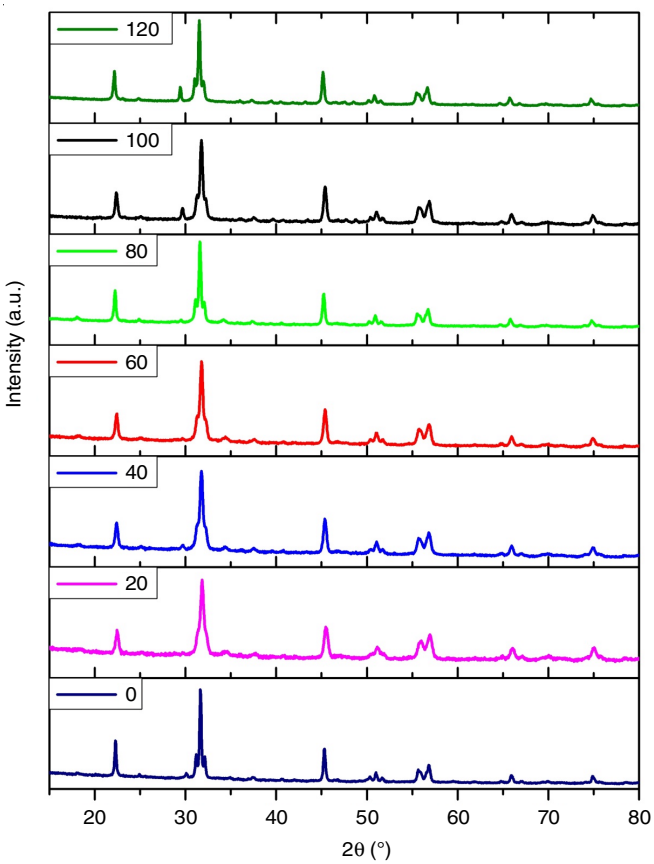

Fig. 1. PXRD patterns of $CaZrO_3:xEu^{3+}$ (x = 0.05) with different nitridation time

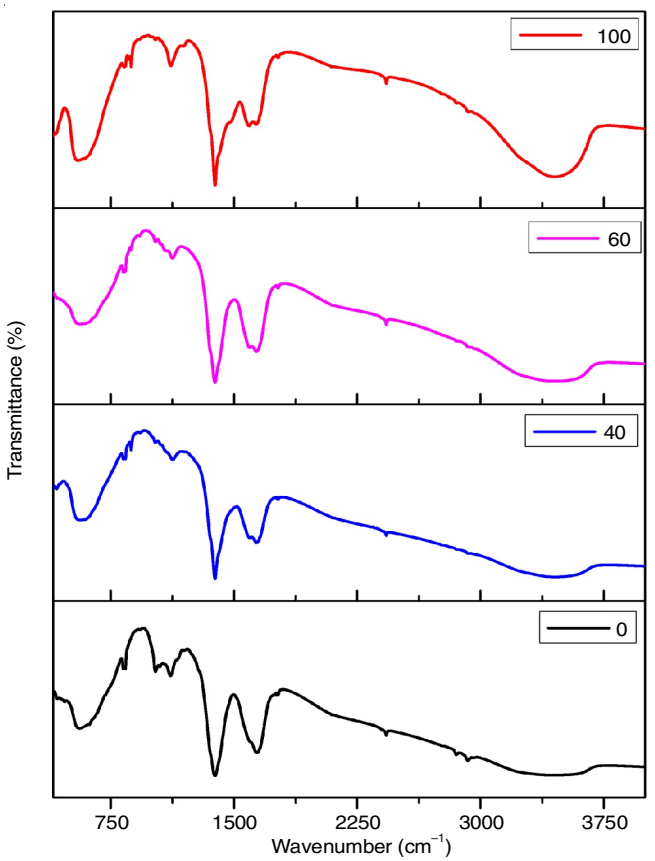

Fig. 2. FTIR patterns of $CaZrO_3:xEu^{3+}$ (x = 0.05) with different nitridation time

materials produced by solution combustion synthesis method. Peaks at ~1400 and ~1115 cm^{-1} were observed as sharp and can be attributed to CO_3^{-2} stretching, These carbon traces maybe due to glycine (organic fuel) post combustion process. The spectra clearly show that no significant absorption variation was observed due to doping of Eu^{3+} as well as N.

SEM analysis: Images from the scanning electron microscopy (SEM) for samples of $CaZrO_3$ are shown in Fig. 3. The micrographs exhibit flakey agglomerations seen to be highly porous as formed. This formation in the material is to be attribute to the method of the synthesis adopted in this work. The gases exited the solution mixture post combustion leaves the highly porous morphology to the synthesized $CaZrO_3$. It has also been reported in majority of the literature on combustion synthesis that this is a common occurrence in the products of this route. The agglomerations observed in this work happen due to the high temperatures aiding sintering of particles and hence resulting in agglomerations. In addition, there was sudden changes in temperatures as the ignition begins reaching a high maximum and quickly ends in a short duration and a decrease in temperature was observed. This is also responsible for the obtained agglomerated mass morphology observed.

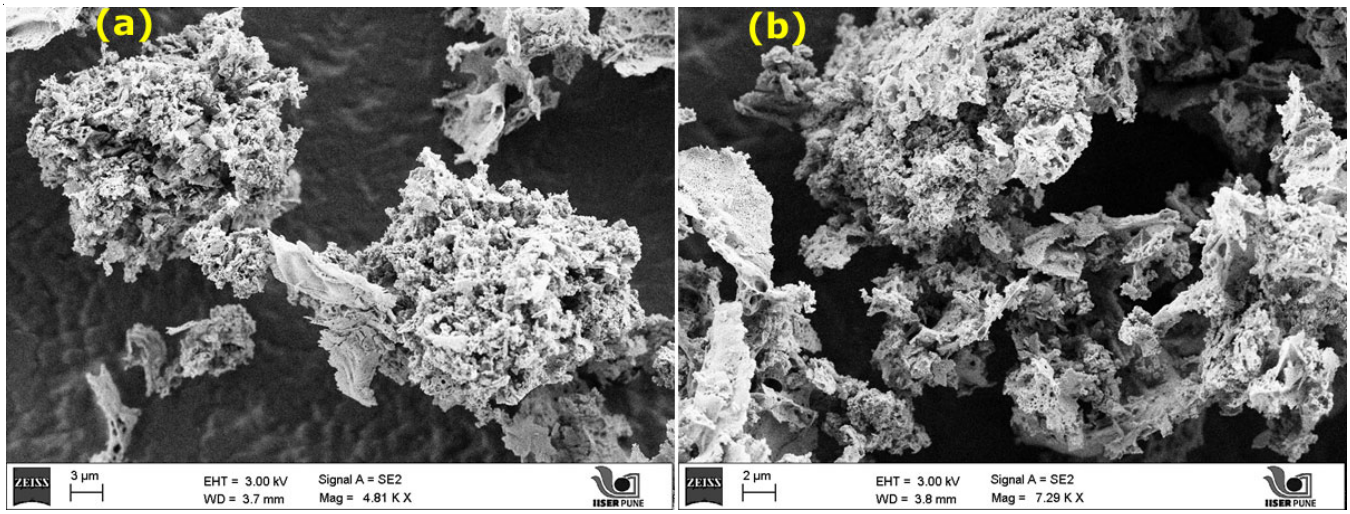

Fig. 3. SEM images of $CaZrO_3:xEu^{3+}$ (x = 0.05) with different magnification

TEM analysis: Transmission electron microscopy (TEM) and high-resolution TEM (HRTEM) is performed to be able to accurately determine the particle size distribution in the as-formed $CaZrO_3$. The image shown in the Fig. 4 exhibits that the average particle size was ~ 40 nm clearly exhibiting that the material falls under the nano regime. It also showed the agglomerated formations of particles owing to the method of preparation adopted.

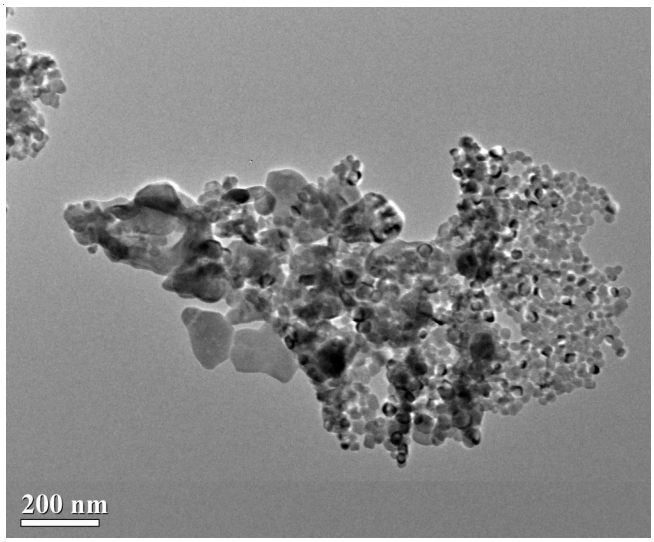

Fig. 4. TEM image of $CaZrO_3:xEu^{3+}$ (x = 0.05)

Photoluminescence emission spectra: The photoluminescence emission spectra for nitrogen doped $Ca_{0.95}Eu_{0.05}ZrO_3$ (N-doping = 0, 20, 40, 60, 80 and 100 min) upon excitated at 272 nm is shown in Fig. 5. Irrespective of the duration of nitridation time all the samples exhibited a sharp and intense peak centered at ~ 615 nm corresponding to characteristic emission of Eu^{3+}. It can also be seen from Fig. 5 that in addition to the band at 615 nm, a well resolved emission bands are also seen at ~ 577, 594, 653 and 690 nm. These can be readily indexed to the *f-f* transition of Eu^{3+} luminophore. The emission peaks at 577, 594 and 653 were due to the transitions $^5D_1 \rightarrow {}^7F_0$, $^5D_0 \rightarrow {}^7F_1$, $^5D_0 \rightarrow {}^7F_3$, respectively. Further, it should also be noted

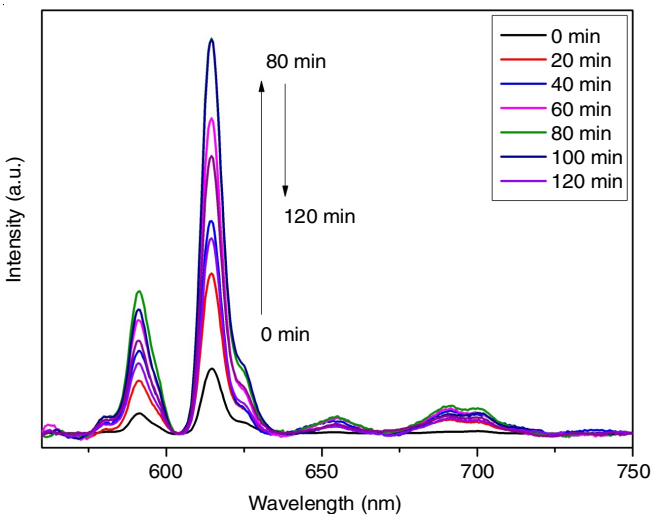

Fig. 5. Photoluminescence emission spectra of $CaZrO_3:xEu^{3+}$ (x = 0.05) with different nitridation time

that no variation in the peak position is observed with varying nitriding time studied. The intensity of the emission peaks were observed to vary as the N-doping concentration changes. It is also clear from the intensity variation plot (Fig. inset) that the emission intensity increases with increase in N-doping time until it reaches a maximum at T = 80 min. Further increase in the time of N-doping was observed to result in the quenching of the emission intensity.

Conclusion

In summary, $Ca_{1-x}ZrO_3:xEu^{3+}$ (x = 0.05) phosphors were successfully prepared by solution combustion method. Powder X-ray diffraction studies confirmed the phase purity and orthorhombic crystal structure of the prepared phosphors. Scanning electron micrographs revealed porous agglomerated morphology. Transmission electron micrographs showed that the prepared samples are in nano regime with particle size ~40-50 nm. The influence of nitridation with varying time intervals showed the effect on the photoluminescenc properties. The photoluminescenc intensity was found to increase with the nitridation upto 80 min and beyond which it decreases.

CONFLICT OF INTEREST

The authors declare that there is no conflict of interests regarding the publication of this article.

REFERENCES

1. C.-H. Huang, T.-M. Chen, W.-R. Liu, Y.-C. Chiu, Y.-T. Yeh, S.-M. Jang, *ACS Appl. Mater. Interf.*, **2**, 259 (2010); https://doi.org/10.1021/am900668r
2. H.R. Abd, Z. Hassan, N.M. Ahmed, M.A. Almessiere, A.F. Omar, F.H. Alsultany, F.A. Sabah and U.S. Osman, *J. Electron. Mater.*, **47**, 1638 (2018); https://doi.org/10.1007/s11664-017-5968-9
3. L. Xiao, R. Wang, Z. Sun, Y. Chen, E. Zhao and L. Liu, *J. Lumin.*, **192**, 668 (2017); https://doi.org/10.1016/j.jlumin.2017.08.001
4. D.L. Monika, H. Nagabhushana, S.C. Sharma, B.M. Nagabhushana and R. Hari Krishna, *Chem. Eng. J.*, **253**, 155 (2014); https://doi.org/10.1016/j.cej.2014.05.028
5. B. Ma and B. Liu, *J. Lumin.*, **188**, 54 (2017); https://doi.org/10.1016/j.jlumin.2017.04.012
6. V.A. Pustovarov, K.V. Ivanovskikh, Y.E. Khatchenko, M. Bettinelli and Q. Shi, *Phys. Solid State*, **61**, 752 (2019); https://doi.org/10.1134/S1063783419050263
7. J. Kaur, V. Dubey, Y. Parganiha, D. Singh and N.S. Suryanarayana, *Res. Chem. Intermed.*, **41**, 3597 (2015); https://doi.org/10.1007/s11164-013-1475-7
8. S. Manjunatha, R. Hari Krishna, T. Thomas, B.S. Panigrahi and M.S. Dharmaprakash, *Mater. Res. Bull.*, **98**, 139 (2018); https://doi.org/10.1016/j.materresbull.2017.10.006
9. M.M. Kumar, R. Hari Krishna, B.M. Nagabhushana and C. Shivakumara, *Spectrochim. Acta A Mol. Biomol. Spectrosc.*, **139**, 124 (2015); https://doi.org/10.1016/j.saa.2014.11.095
10. R. Hari Krishna, B.M. Nagabhushana, B.N. Sherikar, N.S. Murthy, C. Shivakumara and T. Thomas, *Chem. Eng. J.*, **267**, 317 (2015); https://doi.org/10.1016/j.cej.2014.12.102
11. H. Chen, X. Huang, W. Huang and W. Wang, *Optik*, **134**, 78 (2017); https://doi.org/10.1016/j.ijleo.2017.01.023
12. H.A. Höppe, H. Lutz, P. Morys, W. Schnick and A. Seilmeier, *J. Phys. Chem. Solids*, **61**, 2001 (2000); https://doi.org/10.1016/S0022-3697(00)00194-3
13. X. Piao, K. Machida, T. Horikawa, H. Hanzawa, Y. Shimomura and N. Kijima, *Chem. Mater.*, **19**, 4592 (2007); https://doi.org/10.1021/cm070623c

14. S. Yoon, E.H. Otal, A.E. Maegli, L. Karvonen, S.K. Matam, S. Riegg, S.G. Ebbinghaus, J.C. Fallas, H. Hagemann, B. Walfort, S. Pokrant and A. Weidenkaff, *Opt. Mater. Express*, **3**, 248 (2013); https://doi.org/10.1364/OME.3.000248
15. O.M. ten Kate, Z. Zhang, J.R. van Ommen and H.T.B. Hintzen, *J. Mater. Chem. C Mater. Opt. Electron. Devices*, **6**, 5671 (2018); https://doi.org/10.1039/C8TC00885J
16. C. Manjunath, M.S. Rudresha, B.M. Walsh, R. Hari Krishna, B.S. Panigrahi and B.M. Nagabhushana, *Dyes Pigments*, **148**, 118 (2018); https://doi.org/10.1016/j.dyepig.2017.08.036
17. G.R. Gopal and G.K. Reddy, *Optik*, **174**, 234 (2018); https://doi.org/10.1016/j.ijleo.2018.08.047
18. K. Dhanalakshmi, A. Jagannatha Reddy, D.L. Monika, R. Hari Krishna and L. Parashuram, *J. Non-Cryst. Solids*, **471**, 195 (2017); https://doi.org/10.1016/j.jnoncrysol.2017.05.040
19. S.G. Prasanna Kumar, R. Hari Krishna, N. Kottam, P.K. Murthy, C. Manjunatha, R. Preetham, C. Shivakumara and T. Thomas, *Dyes Pigments*, **150**, 306 (2018); https://doi.org/10.1016/j.dyepig.2017.12.022
20. Y.A. Sethi, C.S. Praveen, R.P. Panmand, A. Ambalkar, A.K. Kulkarni, S.W. Gosavi, M.V. Kulkarni and B.B. Kale, *Catal. Sci. Technol.*, **8**, 2909 (2018); https://doi.org/10.1039/C8CY00521D
21. B. Cole, B. Marsen, E. Miller, Y. Yan, B. To, K. Jones and M. Al-Jassim, *J. Phys. Chem. C*, **112**, 5213 (2008); https://doi.org/10.1021/jp077624c